Journal of Alloys and Compounds 504S (2010) S480–S482

Contents lists available at ScienceDirect

Journal of Alloys and Compounds

journal homepage: www.elsevier.com/locate/jallcom

Microstructural investigation of a rapidly solidified Ti–Zr–Fe–Si–Sn–Nb alloy

Z.G. Liu [a,b,c,*], X. Wang [c], X.P. Wang [c], C.J. Zhang [c], L.H. Chai [c], Y.Y. Chen [c]

[a] Key Laboratory of Micro-systems and Micro-structures Manufacturing (Harbin Institute of Technology), Ministry of Education, Harbin 150001, China
[b] State Key Laboratory of Advanced Welding Production Technology, Harbin 150001, China
[c] School of Materials Science and Engineering, Harbin Institute of Technology, Harbin 150001, China

ARTICLE INFO

Article history:
Received 4 July 2009
Received in revised form 13 April 2010
Accepted 16 April 2010
Available online 22 April 2010

Keywords:
Rapid solidification
Ti alloy

ABSTRACT

A rapidly solidified $Ti_{45}Zr_{19}Fe_{20}Si_{10}Sn_4Nb_2$ alloy was prepared by using centrifugal casting and copper mould. Microstructure characterization by using XRD and SEM revealed the formation of refined microstructure on surface layers at surface area with high cooling rate. The refined microstructure shows very high hardness. The current technique of forming "chill zone" of Ti alloy is considered as an alternative to produce novel Ti based alloys with gradient microstructure.

1. Introduction

Over the past decades, numerous new alloys with the capability to form centimeter-scale bulk metallic glasses (BMGs) have been discovered [1]. Although many BMGs exhibit high strength and substantial fracture toughness, they lack ductility and fail in an apparently brittle manner in unconstrained loading geometries [2,3]. This drawback strongly hinders the application of BMGs. People have contributed a lot to overcome this drawback by many means, such as nanoscale secondary phases to form a composite structure of amorphous/nanoscale phases.

Nanostructure has recently been introduced to amorphous alloys in order to enhance the ductility of BMGs due to the existence of ductile crystalline phases in the glass matrix [4]. This leads to the formation of multiphase nanoscale microstructures [4]. A major breakthrough in enhancing plasticity was achieved for BMG/nanostructured composites containing in situ precipitated dendritic phases upon solidification in Zr- and Ti-based alloys [5].

It is well known that dendrites act as obstacles restricting the excessive deformation by isolating the highly localized shear bands in small, discrete inter-dendritic regions, and contribute to the plasticity in many alloy systems. In a recent study [1], it was suggested that microscale ductile crystalline phases might therefore be used to toughen nanostructured materials.

Ti alloys have been considered as the best candidate for hard tissue replacement and implants to human body. Many Ti alloys have been developed for this purpose [6–9]. However, the mechanical property mismatch with human bone and/or tooth strongly hinders its application. In recent years, many Ti-based BMGs have also been developed which exhibit attractive mechanical properties. However, some of them contain toxic elements, such as V, Al, Be, etc. which is not acceptable for biomaterials application. Developing novel Ti alloys without toxic elements is growing a new direction recently. Especially, the idea to produce composites with amorphous/nanostructured and nano/nano structures to improve the mechanical properties put out the research in a new promising way.

In this paper, we present the study on a Ti based alloy $Ti_{45}Zr_{19}Fe_{20}Si_{10}Sn_4Nb_2$. No elements harmful to human body is included. Rapid solidification was carried out using centrifugal casting in copper mould. The microstructural evolution with different cooling rate was studied.

2. Experimental

The alloy ingot of $Ti_{45}Zr_{19}Fe_{20}Si_{10}Sn_4Nb_2$ was prepared by arc-melting pure elements with purities above 99.9% in a Non-Self Consumption Vacuum Melting Furnace under the protection of argon atmosphere. The alloy ingot was remelted four times to ensure the uniformity of chemical composition. The rapid solidified tabular samples were prepared by centrifugal casting into copper mold on a LZ5 centrifugal casting machine. The phase constituents and microstructure of the produced samples were examined by using X-ray diffraction (Riguku D/MAX RB, Cu target, 50 kV/50 mA) and SEM (Hitachi, H-4300). A Vicker's Hardness test was performed to test the overall hardness of the sample (HVS-1000, 200 g/10 s). Nanoindentation was performed to evaluate the mechanical property the rapid solidified alloy on a Nanoindentor XP tester (depth 500 nm).

* Corresponding author at: Key Laboratory of Micro-systems and Micro-structures Manufacturing (Harbin Institute of Technology), Ministry of Education, Harbin 150001, China. Tel.: +86 451 86418802; fax: +86 451 86418802.
E-mail address: zhiguang@hit.edu.cn (Z.G. Liu).

0925-8388/$ – see front matter © 2010 Elsevier B.V. All rights reserved.
doi:10.1016/j.jallcom.2010.04.080

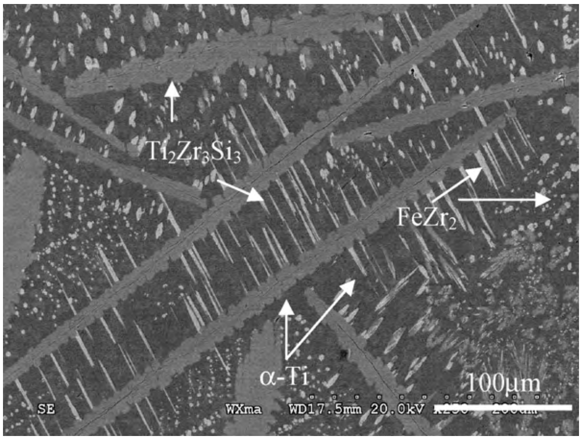

Fig. 1. Microstructure (SEM image) of the arc melted $Ti_{45}Zr_{19}Fe_{20}Si_{10}Sn_4Nb_2$ alloy.

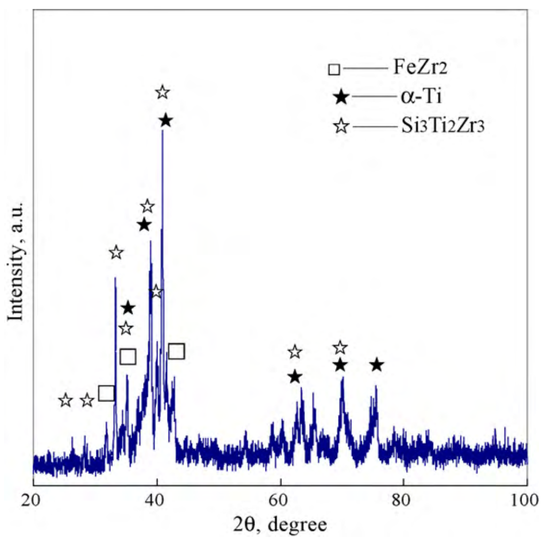

Fig. 2. XRD pattern of the arc melted $Ti_{45}Zr_{19}Fe_{20}Si_{10}Sn_4Nb_2$ alloy.

3. Results and discussions

Fig. 1 shows the microstructure of the arc melted $Ti_{45}Zr_{19}Fe_{20}Si_{10}Sn_4Nb_2$ alloy. It was found that there exist large amount of long columnar crystals in the matrix, together with some small white particle like and rod like phase. The XRD analysis (Fig. 2) revealed that the arc melted alloy consists of α-Ti solid solution, $FeZr_2$ and $Ti_2Zr_3Si_3$ phases. Combining with the EDS analysis, it was indexed that the dark matrix in Fig. 1 is α-Ti solid solution, the bright particle like and rod phase is $FeZr_2$, and the other phase, $Ti_2Zr_3Si_3$. It was also confirmed that Sn tends to dissolve into $FeZr_2$ phase, while Nb dissolves into Ti matrix. The average Vicker's hardness was measured to be 798 ± 9 HV.

Fig. 3. Rapidly solidified $Ti_{45}Zr_{19}Fe_{20}Si_{10}Sn_4Nb_2$ alloy plate, with a size of about 50 × 4 × 1.2.

Fig. 3 shows the rapidly solidified sample plate produced in the present study. The sample size is 50 mm × 4 mm × 1.2 mm. Fig. 4 shows the microstructure (SEM image) of the rapidly solidified $Ti_{45}Zr_{19}Fe_{20}Si_{10}Sn_4Nb_2$ alloy, from one side to the other (thickness: 1.2 mm). The grain refinement by high cooling rate is evidently observed on the surface region of the sample. It was found that in the center region, the microstructure shows similar characteristics as in the arc melted alloy, but with rather finer crystalline grains. The long columnar phase shows length in a range of several tens of micrometers, which is two orders of magnitude smaller than its counterpart in the arc melt alloy. The bright particle-like and rod-like phase was also refined. EDS analysis revealed that the chemical composition of the different phases with different contrasts show similar compositions to their counterparts in the arc melt alloy. The main difference can be observed at the surface area with much higher cooling rate. Much finer microstructure was obtained. Within a depth of 20–30 μm, it was hard to distinguish any crystalline structure. It is believed that the microstructure of the rapidly solidified surface has been refined to sub-miocrometer or even nanometer range. In the region 30–200 μm from the surface, the microstructure is refined significantly as well, but the crystalline phases can be distinguished. In the central region, 200–600 μm from the surface, the microstructure is characterized by relatively coarse grains similar to that in the arc melted sample.

The XRD patterns of the rapidly solidified alloy at different positions are shown in Fig. 5. For comparison, the XRD pattern of the arc melt ingot was presented as well. At the very surface region, the formation of a supersaturated solid solution of Ti-phase was indicated by the shift to higher 2θ value of XRD peaks correspond to α-Ti phase. The peaks corresponding to Fe–Zr and Ti–Zr–Si compound phases are still there. This indicates that rapid solidification promotes the formation of supersaturated solid solution of matrix

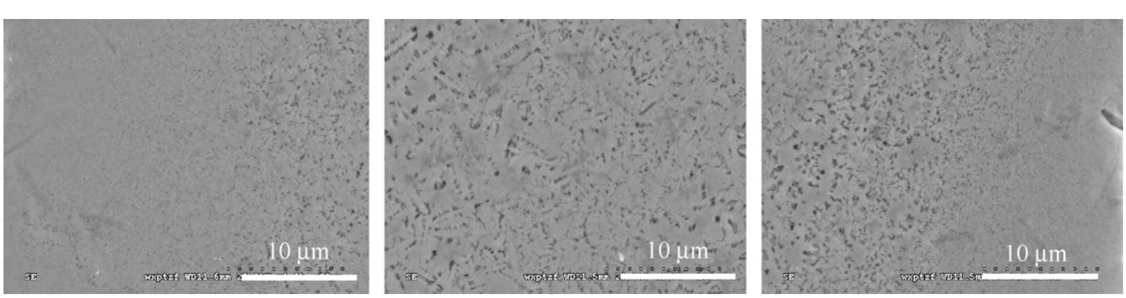

Fig. 4. Microstructure (SEM image) of the rapidly solidified $Ti_{45}Zr_{19}Fe_{20}Si_{10}Sn_4Nb_2$ alloy, from one side to the other (thickness: 1.2 mm). The grain refinement by high cooling rate is evidently observed.

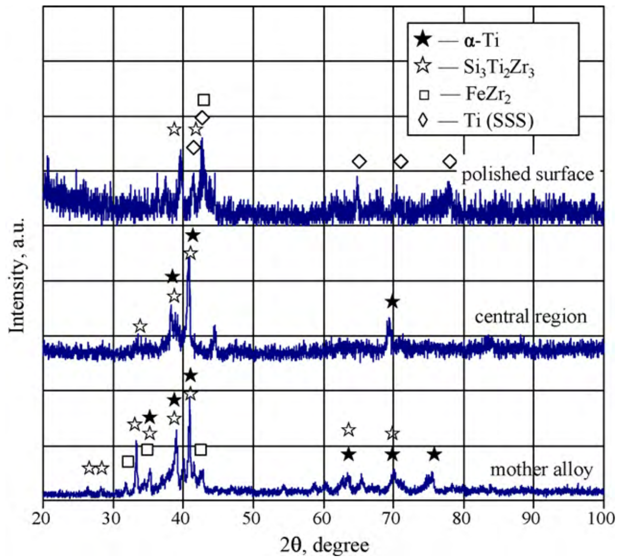

Fig. 5. XRD patterns of the arc melted $Ti_{45}Zr_{19}Fe_{20}Si_{10}Sn_4Nb_2$ alloy, and the corresponding rapidly solidified alloy at different spots: polished surface and central region. The XRD pattern of mother alloy was presented for comparison.

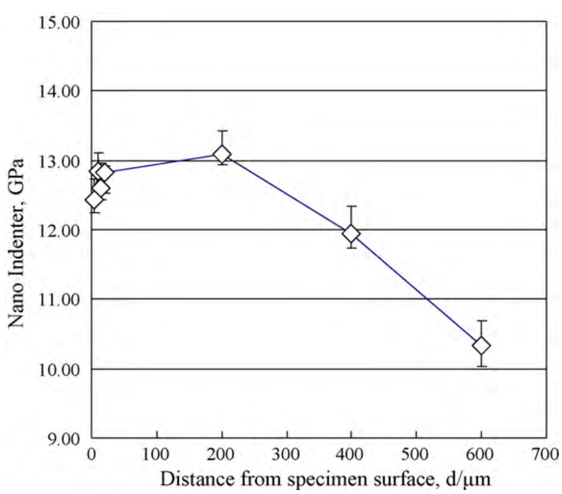

Fig. 6. Hardness measurement via nanoindentation of the rapidly solidified $Ti_{45}Zr_{19}Fe_{20}Si_{10}Sn_4Nb_2$ alloy along with the distance from sample surface.

metal (elements such as Sn, Nb, etc., which do not form compound phase). The XRD pattern for the sample at the central region of the sample, however, shows stronger crystalline peaks similar to those of mother alloy, indicating that crystalline phases with coarser grain size formed.

Nanoindentation tests were also performed to the rapidly solidified $Ti_{45}Zr_{19}Fe_{20}Si_{10}Sn_4Nb_2$ alloy on the cross section of the specimen (see Fig. 6). Test positions was 5, 10, 15, 20, 40, 60, 100, 200, 600 μm from surface. A significantly enhancement of the hardness was observed in the surface region about 0.2 mm from the surface. A slightly lower hardness at the very surface region was attributed to the possible formation of Ti based supersaturated solid solution (shorted as Ti_{SSS}) with some $FeZr_2$ and $Ti_2Zr_3Si_3$ compounds. The increase of hardness in the region under very surface was attributed to the refined structure of α-Ti solid solution, $FeZr_2$ and $Ti_2Zr_3Si_3$ phases. The low hardness at central region measured from nanoindentation, though, is not accurate due to the coarse grains, the tendency of hardness reduction from surface to central region is evident. This hardness change was attributed to the microstructure difference resulted from cooling rate difference. For the melting spinning technique, the estimated cooling rate of melt contacting the copper roll is 10^5–10^7 K/s [10,11]. However, with the increase of distance from the roll surface, the cooling rate decreases at the central point of ingot. Higher cooling rate corresponds quite well to the refined microstructure and higher hardness, while lower cooling rate corresponds to coarser microstructure in the central region of the specimen (see SEM observations) and lower hardness.

The current results in Ti-based alloy are quite similar to so-called “Chill Zone” formed on the surface of undercooled copper alloy [12] and AlNiY alloy [13]. In the copper alloy, a “chill-zone” surface layer 200–300 μm thick with ultrafine eutectic nanostructure composed of fcc-Cu solid solution and Cu_5Zr type intermetallics was obtained and led to dramatic increase in mechanical strength of the small castings. In the undercooled AlNiY alloy, it was found that hard submicron crystalline surface layers of thickness about 200 μm form when the melt was undercooled. A high mechanical strength in excess of 1 GPa was obtained. Both alloys show hard “chill-zone” surface with fine microstructure and high mechanical properties. However, the thickness of the “chill-zone” in Al alloy and Cu alloy was larger than in present Ti alloy. It may be due to the high melting point of Ti alloy, which leads to a thin undercooled region in the melt contacting the cooling copper mould wall. This technique is believed to be a potential way to produce materials with gradient structure and properties from surface to the center.

4. Conclusions

A rapidly solidified $Ti_{45}Zr_{19}Fe_{20}Si_{10}Sn_4Nb_2$ alloy was successfully prepared. Higher cooling rate at the surface of the alloy sample results in the formation of refined microstructure. The refined microstructure shows quite high hardness. The lower cooling rate in the center area leads to the formation of relatively coarser microstructure. The current technique forming “chill zone” may be used to produce novel Ti based alloys with gradient microstructure.

References

[1] G. He, J. Eckert, W. Loser, L. Schultz, Nat. Mater. 2 (2003) 33–37.
[2] X. Rao, P.C. Si, J.N. Wang, Z. Xu, S. Xu, W.M. Wang, W.H. Wang, Mater. Lett. 50 (2001) 279–283.
[3] S.L. Zhu, X.M. Wang, F.X. Qin, A. Inoue, Mater. Sci. Eng. A 459 (2007) 233–237.
[4] C. Pan, A. Inoue, Mater. Trans. JIM 38 (1997) 1040–1046.
[5] Z.F. Zhang, G. He, H. Zhang, J. Eckert, Scripta Mater. 52 (2005) 945–949.
[6] M.F. Lopez, A. Gutierrez, M.C. Garcia-Alonso, M.L. Escudero, J. Mater. Res. 13 (1998) 3411–34166.
[7] M.L. Escudero, M.F. Lopez, J. Ruiz, M.C. Garcia-Alonso, H. Canahua, J. Biomed. Mater. Res. 31 (1996) 313–317.
[8] M.F. Lopez, A. Gutierrez, J.A. Jimenez, Electrochim. Acta 47 (2002) 1359–1364.
[9] M.F. Lopez, J.A. Jimenez, A. Gutierrez, Electrochim. Acta 48 (2003) 1395–1401.
[10] A. Lawley, Ann. Rev. Mater. Sci. 8 (1978) 49–69.
[11] R.E. Anderson, A.R. Cox, T.D. Tillman, E.C. Van Reuth, in: R. Mehrabian, B.H. Kear, M. Cohen (Eds.), Rapid Solidification Processing: Principles and Technologies II, Claitor’s Publishing Division, Baton Rouge, LA, 1980, p. 273.
[12] A.R. Yavari, K. Ota, K. Georgarakis, A. LeMoulec, F. Charlot, G. Vaughan, A.L. Greer, A. Inoue, Acta Mater. 56 (2008) 1830–1839.
[13] Y. Li, K. Georgarakis, S. Pang, J. Antonowicz, F. Charlot, A. LeMoulec, T. Zhang, A.R. Yavari, J. Alloys Compds. 477 (2009) 346–349.